BNL-209092-2018-TECH
CBETA/027

A review of various methods of detecting and measuring beam halos

A. Morris, S. Peggs

August 2018

Collider Accelerator Department
Brookhaven National Laboratory

U.S. Department of Energy
USDOE Office of Science (SC), Nuclear Physics (NP) (SC-26)

DISCLAIMER

A Review of Various Methods of Detecting and Measuring Beam Halos

A. Morris, Oxford University
arthur.morris@ccc.ox.ac.uk

August 21, 2018

Abstract

Halos in high energy particle beams require constant monitoring to minimise beam losses and damage to accelerator components. Four methods of measuring halos are described: wire scanner, laser wire scanner, diamond detector and halo masking monitors. Details of their effectiveness' from tests at various accelerators are used to evaluate how useful they are. It is found that methods making use of wire and laser wire scanners are unable to achieve a high enough dynamic range to measure the outer halo, where the intensity of particles is very low. Diamond detectors can be used to determine the presence of a halo, but are unable to reconstruct their shape. The halo masking method, which makes use of a digital micromirror device to block out high intensity light, produces very good results, but it is possible that light is scattered inside the phosphor screen used to produce an image from the beam, skewing the measurements.

1 Introduction

There is no widely accepted definition of the halo of a particle beam in an accelerator, but it is generally taken to be the low intensity distribution of particles surrounding the main 'core' of the beam. Beam halos are observed in all real particle beams. Due to the complex nature of beam dynamics, the mechanisms that cause halos are not fully understood, but it is known that there are a wide range of contributing factors, for example intrabeam and Touschek scattering [1].

Particles in the halo of a beam cause problems in accelerators. For example, lost particles from a high energy beam can cause damage to beam line components [2]. For this reason, it is very important to minimise the number of particles in the halo in any accelerator.

It is possible to measure how much halo there is on a given beam by relying on auxiliary detectors, such as radiation detectors in magnets. However, this doesn't help to determine the distribution of particles in the beam - what the structure of the halo is - and so does nothing to help with the understanding of what conditions minimise the halo. For this, some sort of dedicated measuring device is required.

The great difference in intensity between the 'core' of the beam and the halo makes it very difficult to measure the halo distribution. The core usually dominates any measurements, making the halo negligible. An everyday example of this is attempting to take a photo of a dark object against a bright background: the high intensity light from the background quickly saturates the CCD pixels in the camera sensor, giving an image where the object is silhouetted. Continuing to collect light after the a pixel is saturated causes charge to overflow to neighbouring pixels, creating defects in the image. The image cannot be exposed for long enough to pick up on fine details of the dark object without greatly overexposing the background and decreasing the image quality.

It is therefore of the utmost importance that detectors have a high dynamic range (the ratio of the greatest to lowest intensity measurements possible at any one time).

In this paper I present and compare a number of methods which have been devised to overcome the challenges described above, to enable accurate measurement of beam halos.

2 Methods of detection

Several papers describe different types of beam halo monitor: wire scanner, laser wire scanner, diamond and halo masking.

2.1 Wire scanner

2.1.1 Principle of operation

A thin metallic or carbon wire in an electron beam captures particles [3]. The most basic method of detecting a beam and its halo is to run such a wire through the beam and measure the current through it as a function of position.

A commercial stepper motor is employed to move the wire head in small increments of distance. An ammeter with high time and current resolution measures the low currents in the beam as the wire is moved across it. The signal from the wire is small due to the low intensity of the electrons from the beam, so requires amplification with a gain of 10 or 100.

Secondary electrons can scatter off the wire; a bias voltage applied to the wire suppresses this effect.

2.1.2 Results

Measurements at the J-PARC Linac fitted to a Gaussian distribution showed good agreement at high relative intensities, but poor at values below 10^{-4}.

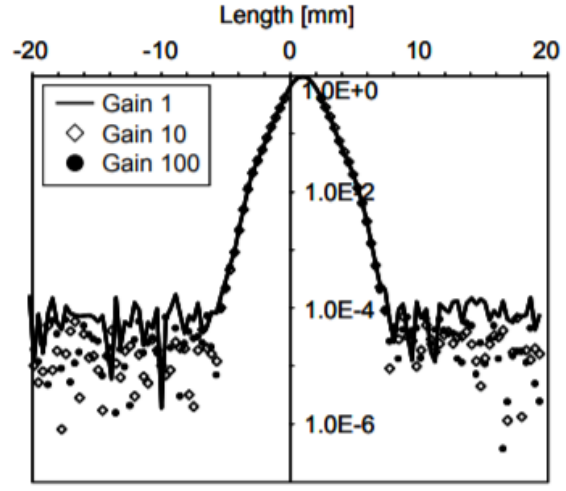

Figure 1: Data from a wire scanner monitor at J-PARC Linac.

At low intensities, noise obscures the signal and limits the maximum achievable dynamic range.

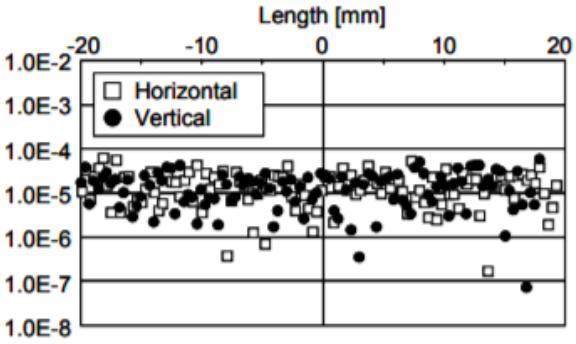

Figure 2: Noise in the J-PARC data.

2.1.3 Drawbacks

As the wire passes through the central region of the beam, the intensity it measures is not just that of the core, but also the halo. The distribution of particles in the beam is not a perfect Gaussian, and in fact varies significantly from beam to beam. It is therefore impossible to determine the intensity of the outer halo compared to just the central region of the beam.

The dynamic range achieved with this setup ($\sim 10^4$) is not high enough to measure the fine details of the outer halo.

2.2 Laser wire scanner

2.2.1 Theory

Compton scattering is the driving principle of the operation of a laser wire beam halo monitor.

When a photon of wavelength λ hits a stationary electron, the particles scatter elastically in a manner similar to that of two colliding billiard balls. Special relativity can be used to describe the energy changes that occur in the collision.

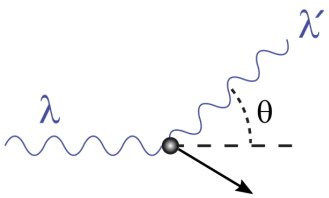

Figure 3: Compton scattering of a photon scattering and a stationary electron.

Using natural units of $c = 1$ the 4-momenta of the electron and photon before and after the collision are

given by

$$\begin{aligned} \mathsf{P}^{\mu}_{e^-,i} &= (m_e,\ \mathbf{0}) \\ \mathsf{P}^{\mu}_{\gamma,i} &= (E_\gamma,\ p,\ 0,\ 0) \\ \mathsf{P}^{\mu}_{e^-,f} &= (E_e,\ \mathbf{p}_e) \\ \mathsf{P}^{\mu}_{\gamma,f} &= \left(E'_\gamma,\ p'\cos\theta,\ p'\sin\theta,\ 0\right). \end{aligned} \tag{1}$$

Rearranging the equation and making use of the invariance of 4-momenta gives

$$\left(\mathsf{P}^{\mu}_{e^-,i} + \mathsf{P}^{\mu}_{\gamma,i} - \mathsf{P}^{\mu}_{\gamma,f}\right)^2 = \left(\mathsf{P}^{\mu}_{e^-,f}\right)^2 \tag{2}$$

which, after simplification, yields the energy of the photon as a function of the angle through which it is scattered

$$\lambda' = \frac{hc}{E'_\gamma} = \lambda + \frac{h}{mc}\left(1 - \cos\theta\right). \tag{3}$$

The Klein-Nishina formula, which can be derived using quantum field theory, gives the differential cross section of the scattering as a function of the incident photon energy and the angle of deflection

$$\mathrm{d}\sigma = \frac{P^2}{2}\left(\frac{\alpha\hbar}{m_e c}\right)^2\left(P + \frac{1}{P} - \sin^2\theta\right)\mathrm{d}\Omega \tag{4}$$

where

$$P = P\left(E_\gamma, \theta\right) = \frac{m_e c^2}{m_e c^2 + E_\gamma\left(1 - \cos\theta\right)} = \frac{\lambda}{\lambda'} \tag{5}$$

and $\mathrm{d}\Omega$ is the differential solid angle.

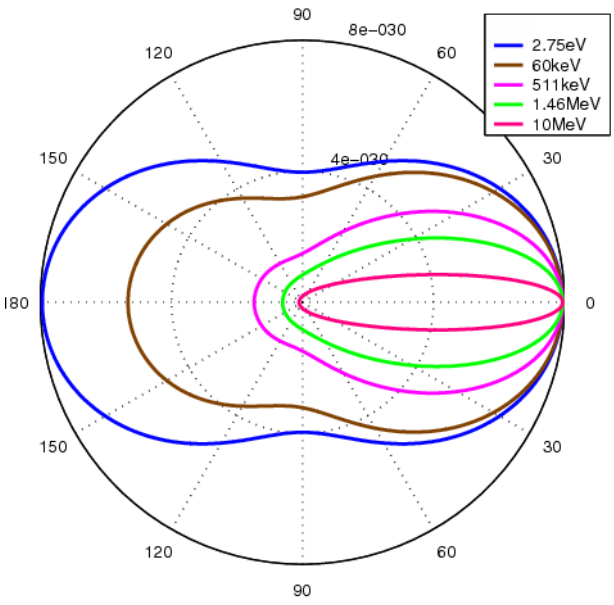

Figure 4: Plots of the Klein-Nishina distribution for a range of common energies.

This equation is valid in the regime where the frequency of the incident photon is relatively low, e.g. visible light.

The appropriate Lorentz transforms can be used to transfer these equations from the frame in which the electron is stationary, to the lab frame.

2.2.2 Principle of operation

A laser wire beam halo monitor shines a laser perpendicular to the beam, and measures the intensity and energy of scattered photons at a given angle. The number of photons that are scattered varies with the number of electrons at the particular point across the beam where the laser shines. Therefore, by moving the laser across the beam and measuring the intensity of scattered light with a scintillator, the distribution of the particles in the beam can be determined.

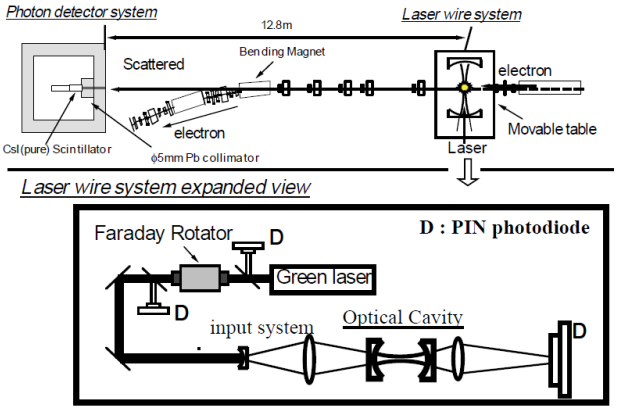

Figure 5: A diagram of the setup

The Klein-Nishina formula predicts that most photons are scattered along the line $\theta = 0$ relative to the electron beam [4], so the scintillator is positioned in line with the beam. The scintillator is placed behind a lead sheet with a hole in it, which acts as a collimator.

An optical cavity placed around the beam forms a Gaussian beam of the fundamental TEM_{00} mode. This is to ensure that the power of the incident photons is constant

Scattered photons are detected by a rectangular $(50 \times 50 \times 100\mathrm{mm}^3)$ scintillator made of a pure caesium iodide crystal.

2.2.3 Results

In the paper by Sakai *et al* [4], the data collected from the KEK accelerator were quite noisy. To try and make some sense of them, the authors made corrections for background radiation and fitted the revised data sets to Gaussian curves.

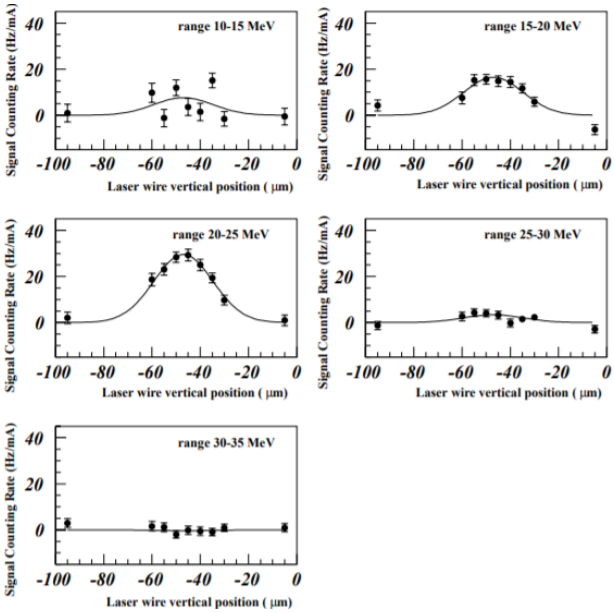

Figure 6: Gaussian fits of the data at several different energy ranges.

Although the fits work well for some plots, the model is generally inconsistent and it is not a particularly accurate method. This is because in reality the distribution of the particles is not normal - it is much more complicated than that.

Using this model, the beam size is $9.8 \pm 1.1 \pm 0.4\mu$m, where the first (second) error represents statistical (systematic) uncertainty.

2.2.4 Drawbacks

As the beam is bent, it emits light in the form of synchrotron radiation at a tangent to the direction of motion of the electrons. This is exactly the same direction that the majority of the photons are scattered in. Although the energy of the synchrotron photons is limited by a maximum value which depends on the beam energy, there is still variation. This radiation is also detected by the scintillator, adding to the noise.

The energy and angle of scattering of the photons also depends on the energy of the electrons in the beam. The paper ignores the fact that not all the electrons in the beam have identical energies; they are also distributed about some mean value. The assumption that all the scattered photons have the same energy is therefore invalid.

Despite being quite a neat idea, in practice using a laser wire to measure beam halo is clearly very impractical and not at all useful.

2.3 Diamond

2.3.1 Principle of operation

Lithography techniques are used to form alumninum electrodes on either side of a thin ($\sim$ 0.3mm) wafer of chemical vapour deposition (CVD) diamond. One electrode applies a voltage bias to the diamond to create an electric field inside it.

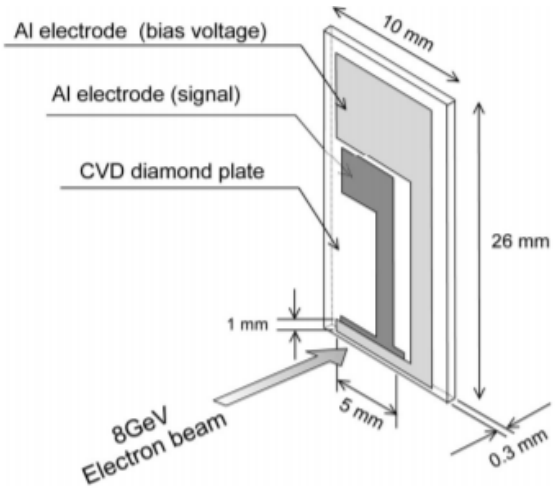

Figure 7: The diamond detector.

When the beam passes through the active area of diamond it creates electron-hole pairs at a rate proportional to the intensity of the beam. In the electric field field these particles move towards either electrode. An electron of 8Gev deposits around 0.1% of its energy in the diamond. The second electrode is connected to an ammeter which measures the current through it. Only a small section (1mm$\times$5mm) on the diamond is sensitive to the beam.

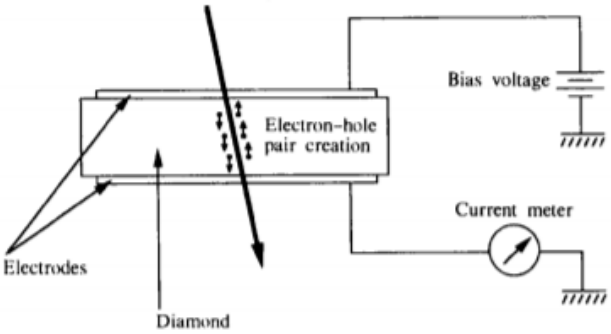

Figure 8: A diagram of particle movement in the detector.

Two such detectors are held, end-to-end, in two clamps. The size of the gap between the detectors is varied with an actuator to change which part of the beam is being measured.

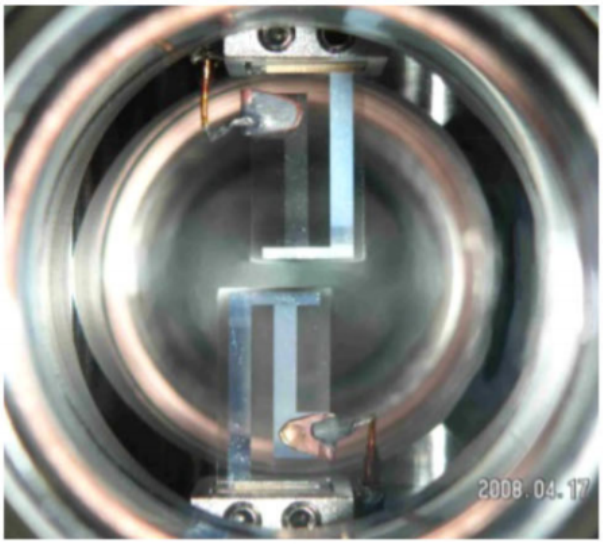

Figure 9: The detector installed in the vacuum chamber at the SPring-8 booster synchrotron.

2.3.2 Results

H. Aoyagi *et al* [5] installed a diamond detector at the SPring-8 booster synchrotron. Pulse-by-pulse measurements were adopted to suppress background noise. The width of the aperture was varied, and the intensity measured by the beam varied accordingly.

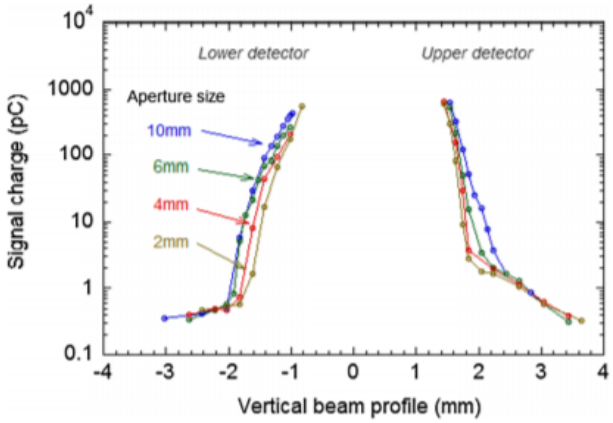

Figure 10: Data from the diamond detector installed at SPring-8.

2.3.3 Drawbacks

The detector can really only be used to determine the presence of a halo. The data which can be collected with a diamond detector are not particularly useful, as they cannot be used to reconstruct the shape of the halo.

Diamond has the desirable properties of very high radiation hardness, high heat resistance and insulation resistance [6]. This component is therefore likely to have a very long lifespan inside the detector. However, aluminium is not so hardy, and the foil electrodes may degrade over time, leading to lower quality performance.

2.4 Halo masking

2.4.1 Principle of operation

A well established and highly effective technique [7] for imaging and measuring the transverse profile of a beam is to place a phosphor screen in the beam line at 90° to the direction of the particles, and use a high resolution CCD camera to image the light emitted. The light produced by the phosphor at any given point is proportional to the number of incident particles. This allows a 2D, rather than just 1D, plot of the beam intensity to be produced.

However, this method is limited by the saturation point of the CCDs in the camera sensor - the point at which one of the pixels is 'full' of charge and can no longer hold any more. The maximum dynamic range achievable is only that of the camera used. Typical CCD cameras do not have a high enough dynamic range to be able to image both the core and the halo simultaneously: the very high intensity core of the beam washes out the images taken by the camera, making it impossible to view the halo.

The method of beam masking [2] can be used to solve this problem.

A digital micro-mirror device (DMD) consists of an array of square mirrors of diameter 16μm, each with two electrodes, one at each of two diagonally opposed corners, which allows the mirror to be angled to $\pm 12°$. The configuration of each individual mirror can be controlled with a computer.

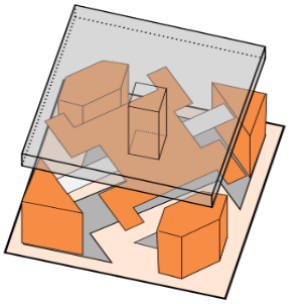

Figure 11: A single micro-mirror.

The idea is to 'mask' the high intensity light from the centre of the beam by using a DMD to direct it away from the sensor. This allows the camera to take a longer exposure photo and capture more fine

detail. In a series of passes the light intensity incident on the sensor is incrementally stepped down, allowing the full image of the beam profile to be built up, with a much higher dynamic range than would otherwise be possible.

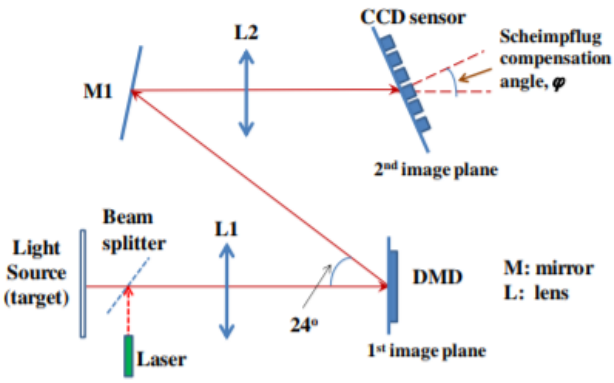

Figure 12: The setup used.

The algorithm for producing a full image is then:

1. Take a photo of the phosphor screen.

2. Use a computer to determine all the pixels which have an intensity above a threshold value. Switch all the corresponding DMD mirrors to direct the light away from these pixels.

3. Repeat until no higher dynamic range image is achieved by successive images i.e. until noise dominates.

Finally, the images are laid on top of one another to produce a single composite image.

The micro-mirrors in a DMD flip along the diagonal, not the horizontal, so the DMD must be put at an angle of 45° to the plane of the rest of the optics.

The sensor must be set at the 'Scheimpflug' angle relative to the light beam to compensate for the angle of the screen in the particle beam. Zhang *et al* show that the required angle is $\varphi = 24.7°$, but also state that in practice a different angle gave them the best images.

The screen is a 31.75 mm diameter glass screen coated with P-43 phosphor ($Gd_2O_2S : Tb$).

2.4.2 Results

Zhang *et al* [2] achieve a dynamic range of 10^7 - higher than any of the other methods.

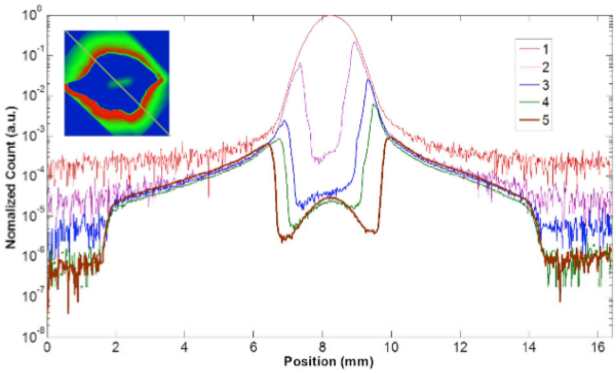

Figure 13: A log-normalised plot of all the successive images.

Figure 7 shows a 'bump' in the middle of the masked section on each of the images. It is particularly noticeable on the highest sensitivity images. This artefact is due to light scattering off the mirrors, so can be simply cut from the data as it known to be irrelevant.

The structure of the reflecting surface of the DMD is highly periodic, and so one might expect incident light to form diffraction patterns, which could affect the quality of the image produced. Zhang *et al* address this issue and find that any diffraction effects are negligible and can be ignored.

2.4.3 Drawbacks

One disadvantage of the DMD method is its insensitivity to time variations in the beam halo. The time required to saturate the CCDs to form an image increases exponentially with each stage, with the longest exposure images taking ~ 50s to capture the very low intensity radiation. The effect of this is a 'motion blur', identical to the blur seen in any normal long-exposure photo. At such low intensities this is virtually unavoidable - if the measurement were only taken over a short periods of time then it would be very difficult to distinguish the signal from random noise.

The method also has the disadvantage that it is destructive - placing a large object in the beam obviously obstructs it.

It is possible to use a very high dynamic range camera, eliminating the need for the DMD system altogether. Some new cameras are (nominally) capable of achieving dynamic ranges of $120 - 150$dB : $10^6 - 10^7$. However, these are extremely expensive and are not at all radiation hard, meaning they would need frequent replacement. This would not be at all economical in the long run.

Zhang *et al* don't consider the possibility that light is scattered in the screen when the beam passes

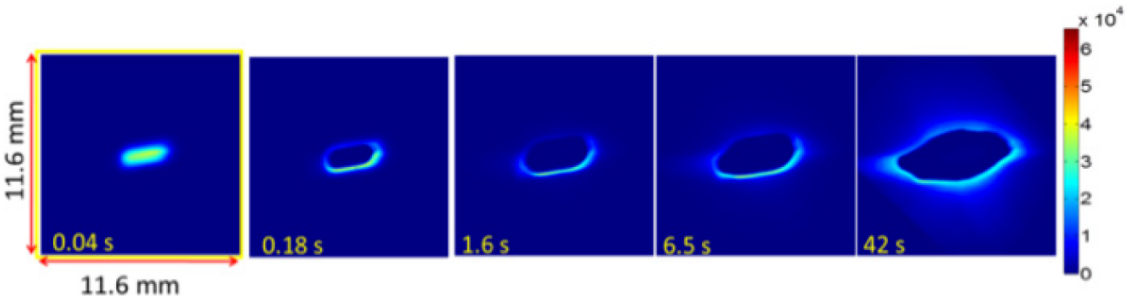

Figure 14: Successive images of the halo

through. This effect could substantially alter the outcome of the measurements, especially considering the extremely low intensities that are measured in the halo.

This issue could be solved by creating a series of phosphor screens with holes to substitute for the regular screen: after measuring the halo of a beam with the normal screen, it could be replaced with one with a hole, and the hole positioned where the centre of the beam was measured to be; when measuring the beam again, the core would pass through the hole and would certainly not be scattered off the screen. This method assumes that the position of the beam is constant across multiple measurements, which may not be the case.

3 Conclusions

The halo masking method is the most useful as it is the only one which allows the full transverse profile of the beam to be imaged rather than simply a one-dimensional trace across it. It also gives the highest dynamic range measurements of any of the methods.

Previous methods of minimising beam halo have relied somewhat on trial and error: through finely adjusting the parameters of the accelerator the radiation detected was sought to be minimised. With the inclusion of a beam halo monitor at several points around the ring the effect of these adjustments could be quantitatively characterised, perhaps giving an insight into *why* the changes help with reducing the radiation.

The installation of one or more such monitors along the beam line would certainly help reduce the time required to diagnose issues with the beam, and would therefore help prevent damage to the accelerator.

References

[1] A Wolski. Space charge, intrabeam scattering and touschek effects. 2009.

[2] H D Zhang et al. Beam halo imaging with a digital optical mask. 2012.

[3] A.Miura et al. Operational performance of wire scanner monitor in j-parc linac. 2010.

[4] H Sakai et al. Measurement of an electron beam size with a laser beam wire profile monitor. 2001.

[5] H Aoyagi et al. Pulse-mode measurement of electron beam halo using diamond-based detector. 2012.

[6] M Friedl. *Diamond Detectors for Ionising Radiation*. PhD thesis, 1999.

[7] S Yencho et al. High resolution screen beam profile monitor. 1985.